Total Neutron Yield from the Reactions $^{13}C(\alpha,n)^{16}O$ and $^{17,18}O(\alpha,n)^{20,21}Ne$†

J. K. Bair
Oak Ridge National Laboratory, Oak Ridge, Tennessee, 37830

and

F. X. Haas
Mound Laboratory, Miamisburg, Ohio

(Received 20 November 1972)

Compound states of high excitation in ^{17}O and $^{21,22}Ne$ have been observed, with good resolution, in the total neutron yield from the reactions $^{13}C(\alpha,n)^{16}O$ and $^{17,18}O(\alpha,n)^{20,21}Ne$. Bombarding α-particle energies were approximately from 1 to 5 MeV. Analysis of the area under the excitation curves gives α-particle strength functions of $\bar{S}_\alpha = 0.029 \pm 0.030$ for $^{13}C+\alpha$, 0.030 ± 0.023 for $^{17}O+\alpha$, and 0.022 ± 0.010 for $^{18}O+\alpha$. For astrophysical purposes these strength functions are used to extrapolate the average cross sections to lower energies.

I. INTRODUCTION

The level structure of ^{17}O has recently been reviewed by Ajzenberg-Selove.[1] Fowler, Johnson, and Feezel[2] and Johnson[2] in their neutron scattering work, have discussed an R-matrix analysis which includes a fit to some of the $^{13}C(\alpha,n)^{16}O$ experimental data obtained in the present work. The $^{18}O(\alpha,n)^{21}Ne$ reaction has been investigated in this energy region by Chouraqui *et al.*[3] who give references to earlier work. No data seem to have been reported on the $^{17}O(\alpha,n)^{20}Ne$ reaction in this energy region. These reactions are not only of interest for the more usual nuclear physics reasons but also may be of astrophysical importance, see, e.g., Refs. 4 and 5. It therefore seemed worthwhile to obtain absolute total neutron-production cross sections with good energy resolution and to extend these measurements down to a reasonably low bombarding energy.

II. EXPERIMENTAL TECHNIQUES

At high energies, the $^4He^+$ beam of the Oak Ridge National Laboratory 5.5-MV Van de Graaff was stripped to $^4He^{++}$ before entering the 90° energy analyzing magnet, and at low energies, the singly charged beam was used directly. Both beams were used in the intermediate region. Bombarding α energies were determined by calibrations based on the $^{19}F(\alpha,n)^{22}Na$ resonance at 2609 ± 3 keV[6] and the $^7Li(\alpha,n)^{10}B$ threshold at 4380 ± 5 keV[7] together with our previous results[8] for $^{18}O(\alpha,n)^{21}Ne$ which were based on the $^7Li(p,n)^7Be$ threshold. During the course of the experiment, the shape of the magnet saturation curve was further studied by observing several sharp resonances with both the singly and doubly charged beams. We estimate that the energy calibration is accurate to ±0.15%.

The analyzed beam impinged on targets placed at the center of the graphite-sphere neutron detector.[9] This detector was recalibrated during the course of the measurements by comparison with a National Bureau of Standards source.

Data were taken both with and without a strong-focus lens between the analyzing magnet and the detector. In the latter case, the slowly diverging beam from the exit slits was collimated by apertures near the magnet in order to form a uniform round spot at the target location. Alignment was continually checked by monitoring possible stray beam current to an aperture very slightly larger than the beam, located near the graphite sphere. In much of the later work an indium vacuum seal was used at the target to aid in preventing carbon buildup; in such cases, an experimentally determined correction was made for the reduction of detector efficiency by neutron capture in the indium.

III. $^{13}C(\alpha,n)^{16}O$

Figure 1 shows the neutron yield obtained by bombarding an infinitely thick disk of compressed carbon enriched in ^{13}C. The nonresonant yield has been subtracted. The curve is the integrated Breit-Wigner yield for the parameters $E_r = 1056.3$ keV and $\Gamma_{exp} = 2.0$ keV. Figure 2 shows similar measurement of the "doublet" at 1.34 MeV, which was previously resolved only in the $^{16}O+n$ data of Johnson and Fowler.[10] Here the curve is the sum of two simple Breit-Wigner shapes using $E_r = 1336.7$ keV with $\Gamma_{exp} = 1.0$ keV for the lower-energy resonance and 1340.6 keV with $\Gamma_{exp} = 1.2$ keV for the upper resonance. Similar, although less detailed measurements, were made on a disk of reactor grade graphite. The average of

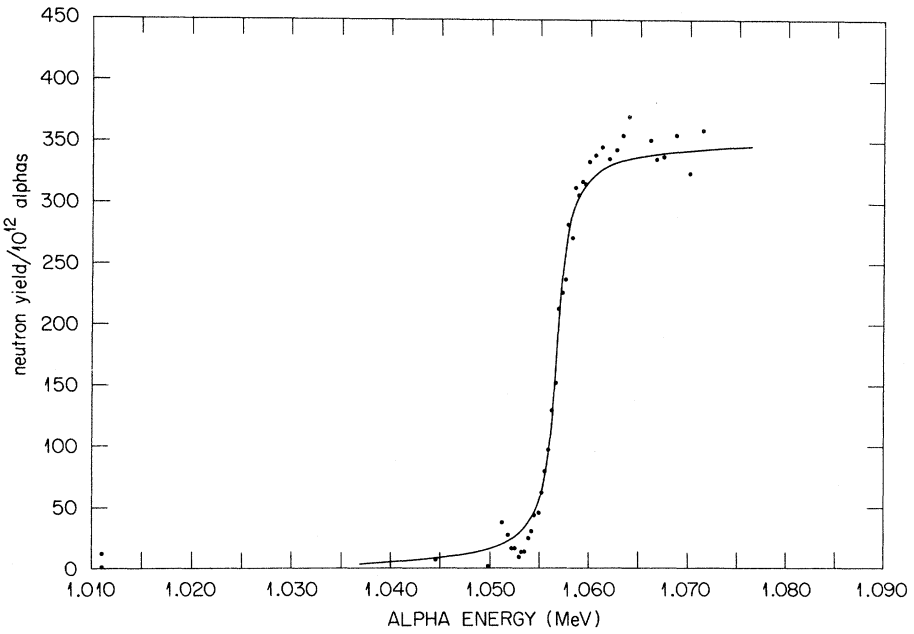

FIG. 1. The data shown were obtained using as target a pressed slug of enriched elemental carbon-13. The background and nonresonant yield have been extracted. The solid curve is the integrated yield of a single Breit-Wigner resonance at 1.0568 MeV having a width $\Gamma = 2.0$ keV in the laboratory system. The error in Γ is estimated as ± 0.2 keV. Note that this is the experimental width and includes beam resolution.

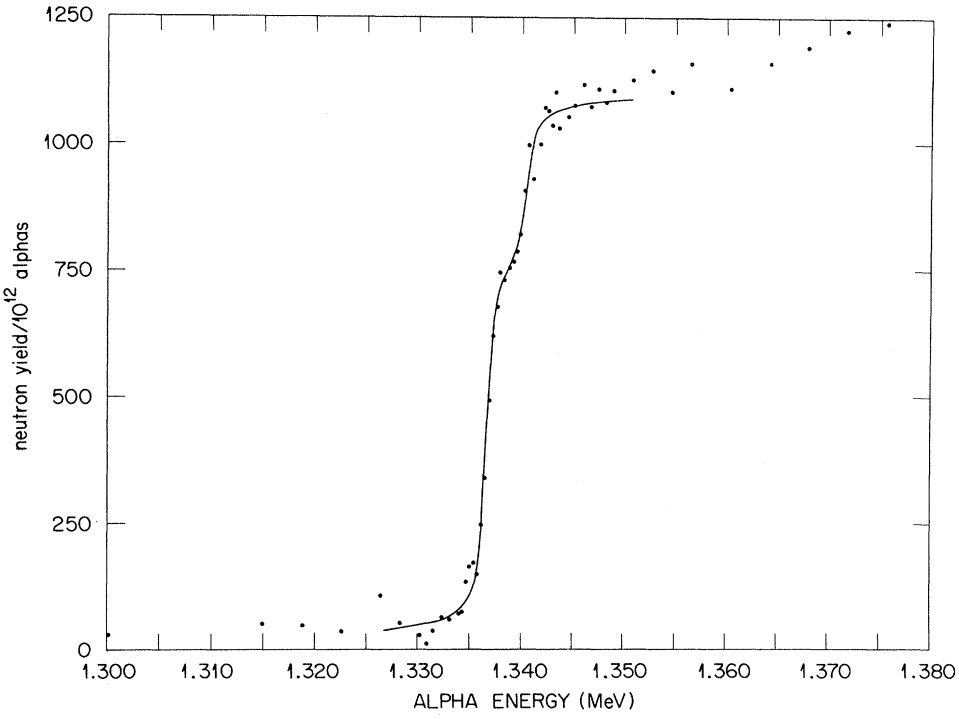

FIG. 2. The data shown were obtained using as target a pressed slug of enriched elemental carbon-13. The background and nonresonant yield have been extracted. The solid curve is the integrated yield of the sum of two Breit-Wigner resonances having assumed resonant energies and widths of 1.3367 MeV, $\Gamma = 1.0$ keV, and 1.3406 MeV, $\Gamma = 1.2$ keV (lab system). The errors in the widths are estimated to be ± 0.1 keV for the lower resonance and ± 0.2 keV for the upper resonance. Note that these are experimental widths and include beam resolution.

these measurements yields a step in the yield curve at the 1.06-MeV resonance of 4475 ± 5% neutrons per particle μC, converted to a basis of 100% carbon-13. Using the value of the energy loss of 39.2×10^{-15} eV cm^2 given by Whaling[11] (this value is about 10% lower than that of Palmer[12] and about 10% higher than that of Porat and Ramavataram[13]) one obtains a value of $\sigma_r\Gamma = 17.9$ keV mb ± 10%. From the fit of the calculated curve to data such as Fig. 1 we estimate the error of Γ_{exp} as less than 10%. When the correction for beam resolution is made we find $\Gamma = 1.9$ keV ± 10%. Finally, the resonant cross section is $\sigma_r = 9.4$ mb ± 15%. In a similar way we can obtain the values of 36.8 and 15.9 keV mb for $\sigma_r\Gamma$ for the 1336.7- and 1340.6-keV resonances, respectively. The corresponding cross-section values are 46 and 17 mb, respectively, with an error of 18% in both cases.

Figure 3 shows a yield curve obtained with a thin (5 keV at 1 MeV) ^{13}C target produced by cracking enriched acetylene onto a platinum backing. The cross-section scale is based on the thick target measurements as discussed above and are estimated to be reliable to ±20% for structure suitably wider than the target thickness. Table I lists the energies of the maxima of the yield with corresponding excitation energies in ^{17}O (based on $E_{ex} = 0.764\,65E_\alpha + 6357.0$) as well as estimated resonant widths. The values given are best values obtained from several measurements and are in excellent agreement with those obtained from other work; see Ref. 2. Kerr, Morris, and Risser[14] have pointed out that their energies, for α energies above about 4 MeV, disagree by

TABLE I. Level parameters for ^{13}C + α. Shown are the incident α-particle energy, the energy of excitation in the ^{17}O compound system, and the total width in the center-of-mass system.

E_{lab} (keV)	E_{ex} (keV)	$\Gamma_{c.m.}$ (keV)	E_{lab} (keV)	E_{ex} (keV)	$\Gamma_{c.m.}$ (keV)
1056.3	7164.7 ± 1.5	1.5 ± 0.2	3415	8968 ± 4	14
1336.7	7379 ± 1.5	$0.6^{+0.2}_{-0.1}$	3645	9144 ± 4	9
1340.6	7382 ± 1.5	$0.8^{+0.3}_{-0.2}$	3714	9197 ± 4	8
1590	7573 ± 2	≤1	4096	9489 ± 4	16
1745	7691 ± 6	≤15	4394	9717 ± 5	25
2083	7950 ± 8	75	4465	9771 ± 15	~25
2250	8077 ± 8	110	4583	9861 ± 5	14
2407	8198 ± 8	70	4600	9874 ± 15	~10
2604	8348 ± 4	15	4730	9974 ± 20	~80
2680	8406 ± 3	8	4820	10 043 ± 20	~100
2765	8471 ± 3	8	4993	10 175 ± 5	45
2809	8505 ± 3	6	5200	10 333 ± 15	150
3059	8696 ± 5	50	5325	10 429 ± 10	23
3318	8894 ± 8	115			

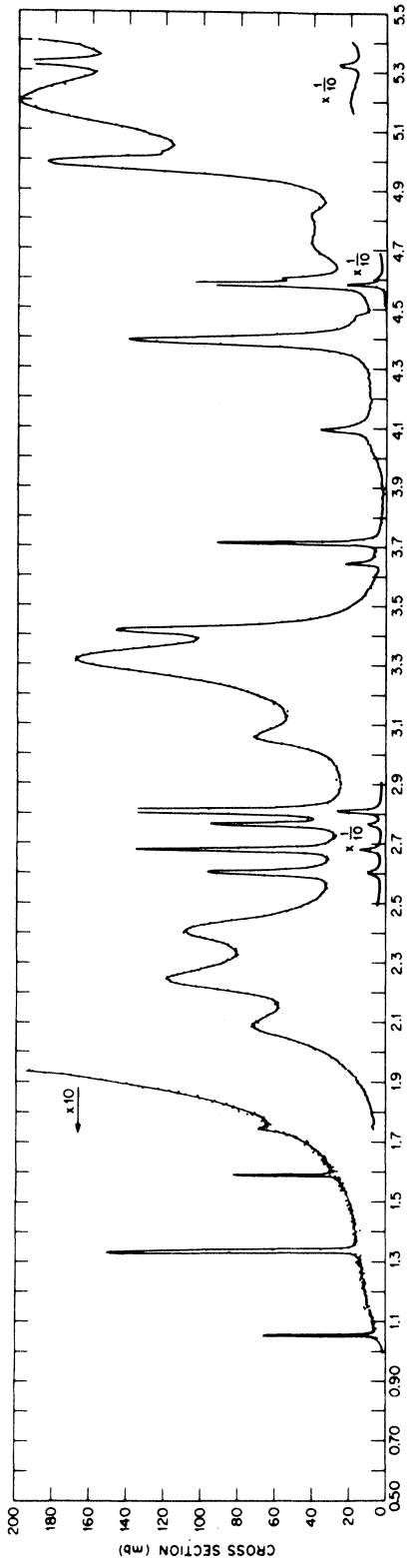

FIG. 3. These data show the ^{13}C(α,n)^{16}O total neutron cross section. The target consisted of a layer of cracked (enriched) acetylene on a platinum backing. The target thickness was measured to be approximately 5 keV at the 1.057-MeV resonance. The energies are in the laboratory system and are corrected for target thickness. The cross-section scale is based on measurements made on the 1.057-MeV resonance using infinitely thick targets, of both enriched and natural elemental carbon, in conjunction with thin target measurements over this resonance and the wide resonance at about 2.4-MeV energy.

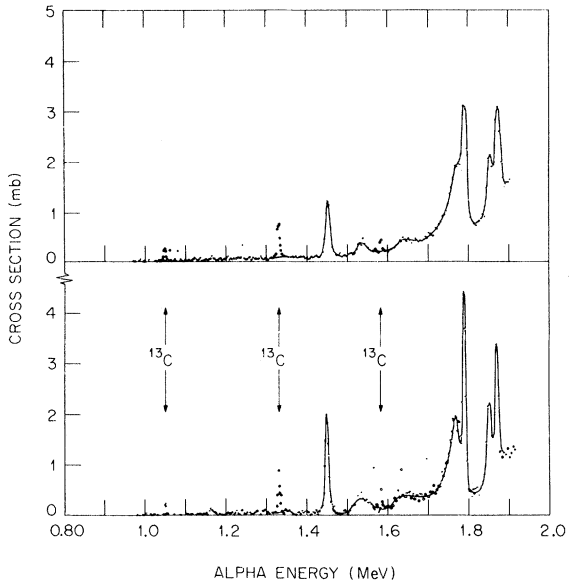

FIG. 4. The data shown here were taken with targets made by anodizing tantalum disks in water enriched to 15.7 at.% ^{17}O and 5.0 at.% ^{18}O. The cross-section scale was obtained by normalizing to the known ^{18}O cross section; it applies only to peaks due to ^{17}O. The top data were taken with a target 13 keV thick for $2\frac{1}{2}$-MeV α particles while the target for the bottom set of data was 6 keV thick at the same energy. The energies are in the laboratory system and have been corrected for target thickness.

as much as 70 keV with those of earlier work[15, 16]: The present data agree with those of Kerr, Morris, and Risser and with those of Robb, Schier, and Sheldon[17] in the region of overlap. Perhaps it should be stressed that the energies of the maxima listed in Table I may, because of interference between levels of the same spin and parity, differ from the true resonant energy. Johnson[2] defines and determines level energies from an R-matrix analysis of neutron-scattering data and part of our (α, n) data. In the cases investigated here, the differences are less than the errors in the measurement. Johnson also gives α-particle widths from his analysis.

The various values of the measured total absolute (α, n) cross section[15, 18] (and those derived from the inverse reaction) are not in really good agreement with each other and are in many cases 20 to 40% below those reported here. Detailed comparisons are, however, difficult to make because of the widely different resolutions involved. On the other hand, if one normalizes the angular distribution of the 5.0- (4.995-) MeV resonance as given by Robb, Schier, and Sheldon[17] to the 0° cross section of Kerr, Morris, and Risser[14] and integrates to get the total cross section, one obtains a value some 15% above that of the present work.

Note added in proof: Thick carbon target yields calculated from the thin target data given here

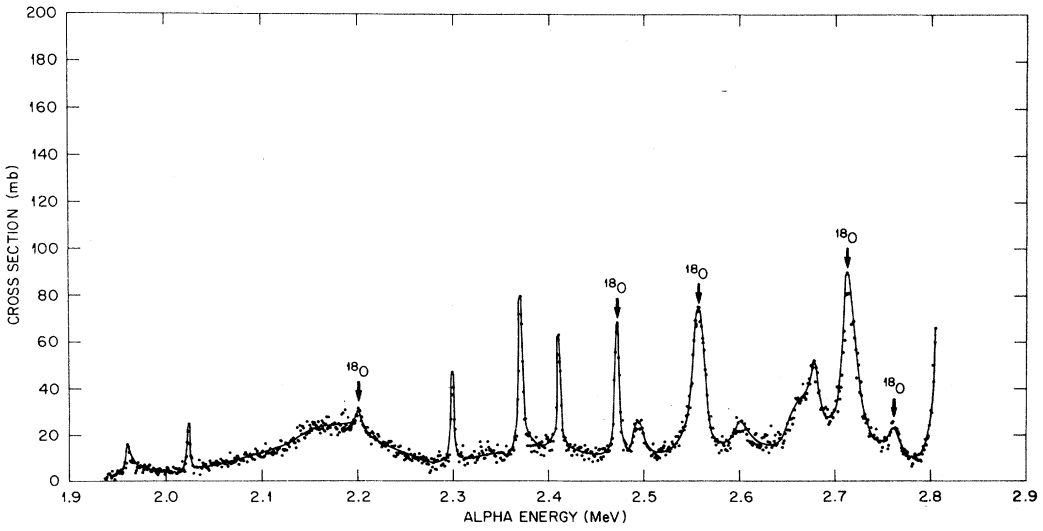

FIG. 5. The data shown were obtained by bombarding a tantalum blank which had been anodized at 4 V in water enriched to 15.7 at.% ^{17}O and 5.0 at.% ^{18}O. The target thickness is ~$2\frac{1}{2}$ keV for 2.5-MeV α particles. The cross-section scale was obtained by normalizing to the known ^{18}O cross section; it applies only to peaks due to ^{17}O. Energies are in the laboratory system and have been corrected for target thickness.

must be reduced by 15 or 20% in order to match smoothly with recent thick target measurements made using α-particle beams of from 5.2- to 9.0-MeV energy (see Bair[18a]).

IV. $^{17}O(\alpha,n)^{20}Ne$

Figure 4 shows the neutron yield measured using targets obtained by anodizing tantalum blanks in water enriched to 15.7 at.% ^{17}O and 5.0 at.% of ^{18}O. The top data were taken with a target 13 keV thick for 2.5-MeV α particles and the bottom with a 6-keV-thick target. The cross-section scale has been determined by normalizing to the ^{18}O resonances[8] at 2.56 and 2.71 MeV and taking into account the known ratio of ^{17}O to ^{18}O enrichment. Figure 5 shows similar data from about 1.9 to 2.8 MeV taken with a target approximately $2\frac{1}{2}$ keV thick for 2.5-MeV α particles.

Figure 6 shows the neutron yield measured using a "drive-in" target[19] made by bombarding a tantalum disk with 24-keV ^{17}O ions. The feed gas had been previously enriched to 15% ^{17}O. Such targets of the noble gases have been studied in considerable detail by Selin, Arnell, and Almen.[20] Their work leads us to expect that the density of drive-in atoms rises very rapidly to a maximum, as a function of distance into the target, and then falls off much more slowly. Selin, Arnell, and Almen give an estimate for the thickness of any possible inert surface layer of tantalum which converts to $\leq$1.5 keV for 2-MeV α particles. Measurements made with thin anodized ^{17}O-^{18}O targets (on the same cycle of the analyzing magnet) gave the experimental widths of the 1.96- and 2.03-MeV resonances as 5.0 and 2.5 keV, respectively, and their separation as 63.5 keV. If we assume that the drive-in targets are infinitely thick for the 2.03-MeV resonance and that there is no straggling of any inert surface layer, we obtain a level width of 2.0 keV in good agreement with the value obtained from the known anodized target thickness. By measuring the lower resonance with a thin anodized target and the upper resonance with a drive-in target, all on the same magnet cycle, we determine that the separation in energy of the levels is the same as that determined above. We therefore conclude that the thickness of any inert surface layer is 0 ± 1 keV. From the fact that the shape of the distribution of ^{17}O is simply related to the shape of the yield curve of a narrow resonance, we estimate that the full thickness at half maximum of the target used to obtain the data of Fig. 6 is 26 keV for 2-MeV α particles. The bombarding energies of Fig. 6 have been corrected by subtracting half of the target thickness. The energies and cross sections

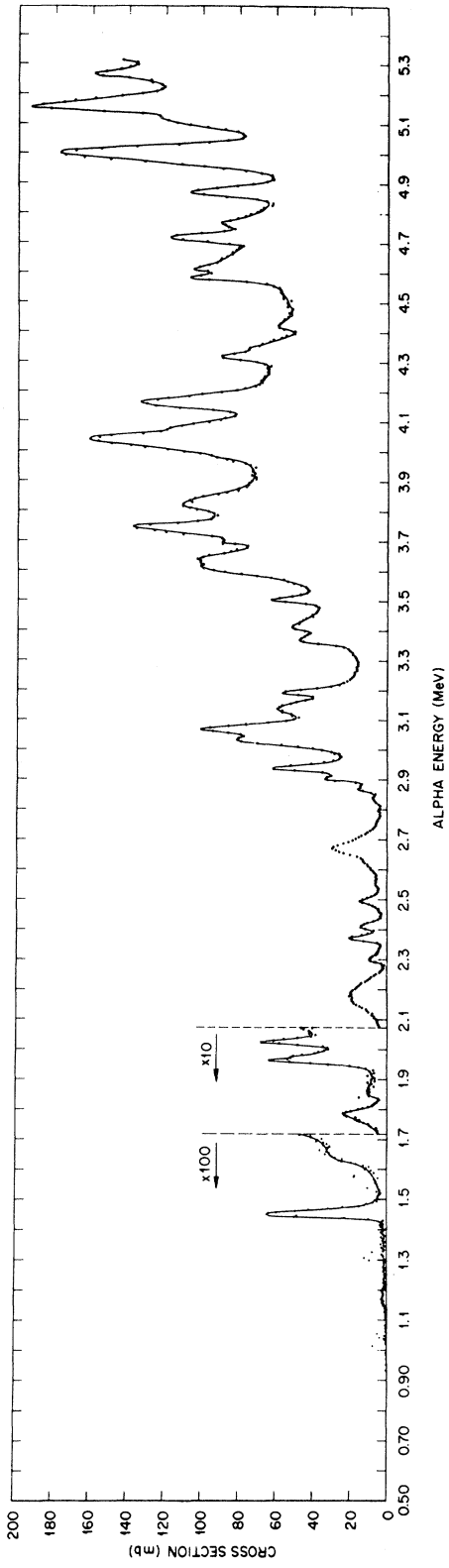

FIG. 6. These data were obtained by means of "drive-in" targets made by bombarding a tantalum blank with 24-keV ^{17}O ions in a magnetic separator. The feed gas had previously been enriched to 15.2 at.% ^{17}O. The target thickness is ~35 keV at 1 MeV. The cross-section scale has been obtained by normalizing to the anodized target data. Energies are in the laboratory system and have been corrected for target thickness.

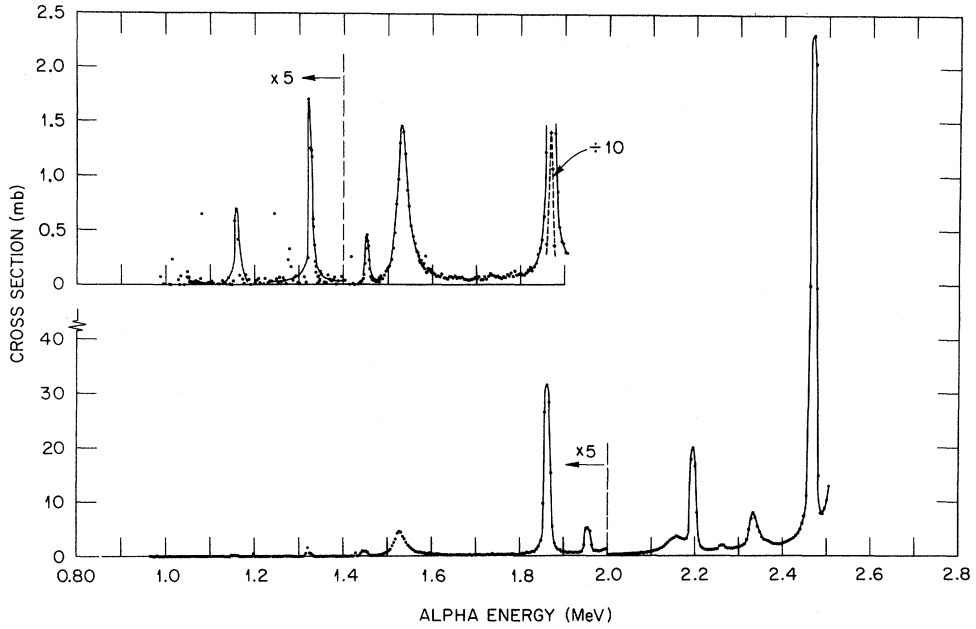

FIG. 7. The data shown in the lower curve were taken with a target mady by anodizing a tantalum blank at 22 V in water enriched to 97 at.% ^{18}O. Target thickness was 13 keV for 2.5-MeV α particles. The inset curve was taken with a similar target having a thickness of only 6 keV. The cross-section scale was obtained by normalizing to the known ^{18}O cross section. Energies are in the laboratory system and have been corrected for target thickness.

TABLE II. Shown are the incident α-particle energies corresponding to maxima in the $^{17}O(\alpha, n)^{20}Ne$ yield curve, the corresponding energy of excitation in the ^{21}Ne compound system, and an estimate of the laboratory width (corrected for target thickness).

Level	E_α (keV)	E_{ex} (keV)	Γ (keV)	Level	E_α (keV)	E_{ex} (keV)	Γ (keV)
1	1452	8524 ± 2	6	25	3190	9931 ± 10	15
2	1535	8591 ± 10	45	26	3370	10076 ± 10	<5
3	1650	8684 ± 10	60	27	3412	10110 ± 10	45
4	1770	8781 ± 5	50	28	3505	10186 ± 10	15
5	1791	8798 ± 2	<5	29	3630	10287 ± 25	80
6	1850	8846 ± 5	10	30	3700	10344 ± 20	≈5
7	1870	8862 ± 5	7	31	3750	10384 ± 10	45
8	1960	8927 ± 5	5	32	3825	10445 ± 15	55
9	2025	8988 ± 5	2.5	33	4040	10619 ± 10	65
10	2175	9109 ± 15	100	34	4165	10720 ± 10	45
11	2300	9210 ± 5	10	35	4320	10845 ± 10	20
12	2370	9267 ± 5	15	36	4360	10878 ± 20	30
13	2410	9299 ± 5	10	37	4425	10930 ± 10	35
14	2495	9368 ± 5	30	38	4585	11060 ± 10	≈5
15	2605	9457 ± 10	35	39	4612	11082 ± 10	<5
16	2665	9506 ± 15	50	40	4620	11088 ± 20	≈100
17	2678	9516 ± 5	20	41	4720	11169 ± 10	30
18	2840	9647 ± 10	30	42	4770	11210 ± 15	25
19	2870	9672 ± 20	≈5	43	4870	11291 ± 10	30
20	2900	9696 ± 10	10	44	5000	11396 ± 10	55
21	2935	9724 ± 10	10	45	5110	11485 ± 25	15
22	3030	9801 ± 15	10	46	5160	11525 ± 15	55
23	3070	9834 ± 10	50	47	5270	11614 ± 15	30
24	3140	9890 ± 15	50				

TABLE III. Level parameters for $^{18}O+\alpha$. Shown are the incident α-particle energies, corresponding excitation energies in the ^{22}Ne compound-compound nucleus, and laboratory widths corrected for target thickness.

Level	E_α (keV)	E_{ex} (keV)	Γ (keV)
1	1159	10615 ± 3	6
2	1322	10749 ± 3	6
3	1450	10853 ± 3	6
4	1530	10919 ± 3	24
5	1864	11192 ± 3	7
6	1955	11266 ± 5	12
7	2160	11434 ± 8	48
8	2195	11463 ± 3	≤3
9	2335	11577 ± 5	18
10	2467	11685 ± 5	9

are correct only for levels whose widths are greater than the target thickness.

The $^{17}O(\alpha, n)^{20}Ne$ data of Figs. 4, 5, and 6 have not been corrected for the variation of graphite-sphere detector efficiency as a function of neutron energy since the energy spectrum of the neutrons is unknown. This correction would be negligible at the lower energies but might be as much as +5% at our highest bombarding energies. Exclusive of this, the over-all error is estimated as ±25%.

Table II lists "level" parameters. For α-particle energies below about 2.8 MeV these data are taken with the anodized target. Above this energy the data are taken with the drive-in target and narrow resonances would not be resolved. Thus above 2.8 MeV it would be unwise to attempt to

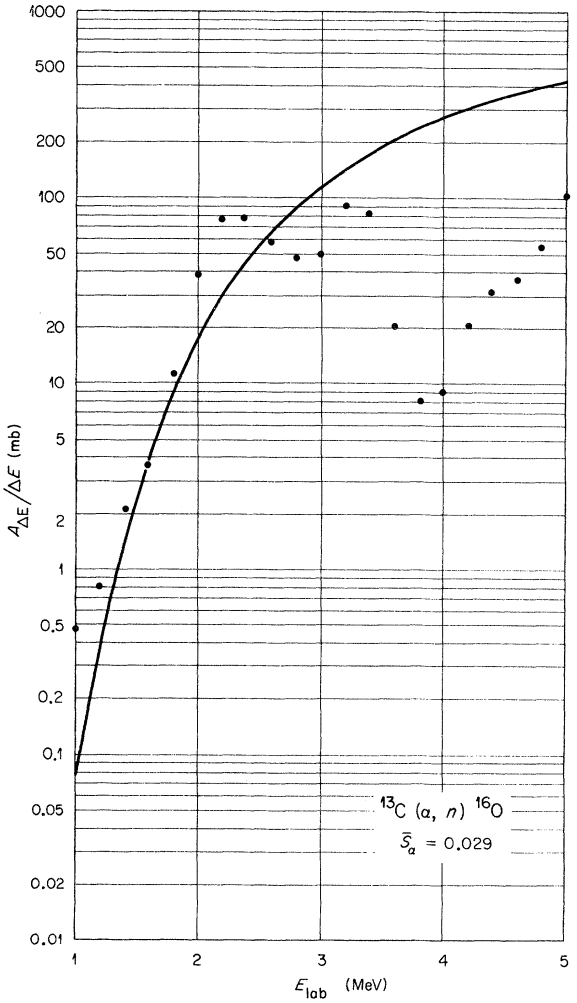

FIG. 8. Plot of $A_{\Delta E}/\Delta E$ as a function of incident α-particle energy for the reaction $^{13}C(\alpha,n)^{16}O$. Here $A_{\Delta E}$ is the area under the excitation curve in the energy region ΔE. The solid curve is calculated based on an α-particle strength function $\bar{S}_\alpha = 0.029$.

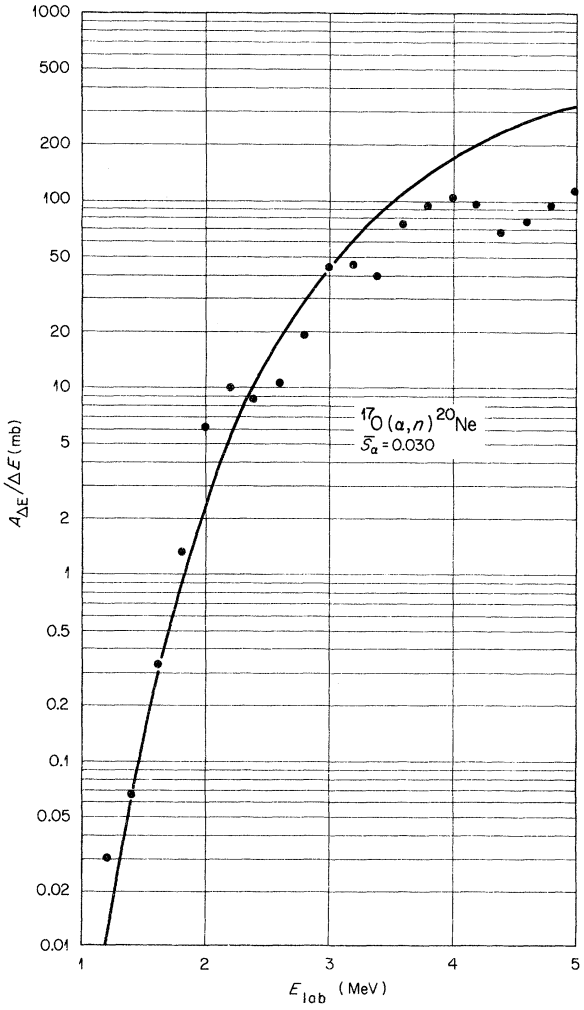

FIG. 9. Plot of $A_{\Delta E}/\Delta E$ as a function of incident α-particle energy for the reaction $^{17}O(\alpha,n)^{20}Ne$. $A_{\Delta E}$ is the area under the excitation curve in the energy region ΔE. The solid curve is calculated based on an α-particle strength function of $\bar{S}_\alpha = 0.030$.

closely correlate the structure of the yield curve to level structure in the compound nucleus. Excitation energies are based on $E_{ex} = 0.809\,42E_\alpha + 7348.7$.

V. $^{18}O(\alpha,n)^{21}Ne$

We have previously reported[8] the total neutron yield from this reaction for bombarding energies greater than 2.5 MeV. With the better techniques now available, it was possible to extend these data down to much lower energies. Figure 7 shows such data taken with an anodized ^{18}O target 13 keV thick for 2.5-MeV α particles and also (inset) with a 6-keV target. The cross-section scale has been obtained by normalizing to the older data, the estimate of the error remains ±25%. Table III gives the level parameters. Excitation energies are based on $E_{ex} = 0.818\,08E_\alpha + 9667.0$.

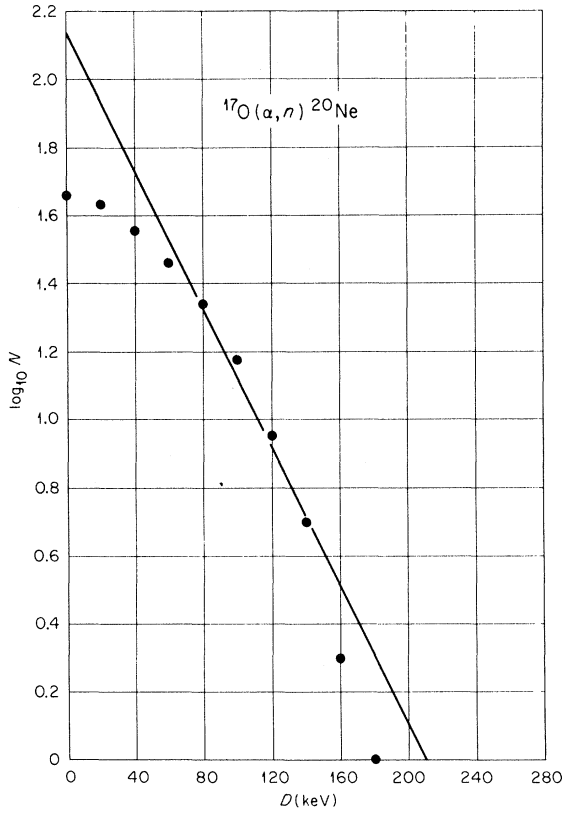

FIG. 10. Plot of the log of the number of levels in $^{17}O(\alpha,n)^{20}Ne$ having a spacing greater than some spacing D. The intercept corresponds to a total of 138 levels of which we observe 47. The slope corresponds to a level spacing of 43 keV to be compared to our experimental value of 81 keV.

VI. DISCUSSION

A. $^{13}C(\alpha,n)^{16}O$

Following the techniques used in previous work at this laboratory,[8,21] we have averaged the $^{13}C(\alpha,n)^{16}O$ cross-section data over an interval region ΔE of 400 keV and plotted the area under the yield curve per unit ΔE as a function of the incident α-particle energy. These data are shown as the points in Fig. 8. If we assume (1) that $\Gamma_n \gg \Gamma_\alpha$ and that all other widths are negligible [the (α,p) reaction has a $Q = -7.4$ MeV] and (2) that the net effect of interference terms in the total cross section is zero when averaged over the levels, we can define an α-particle strength

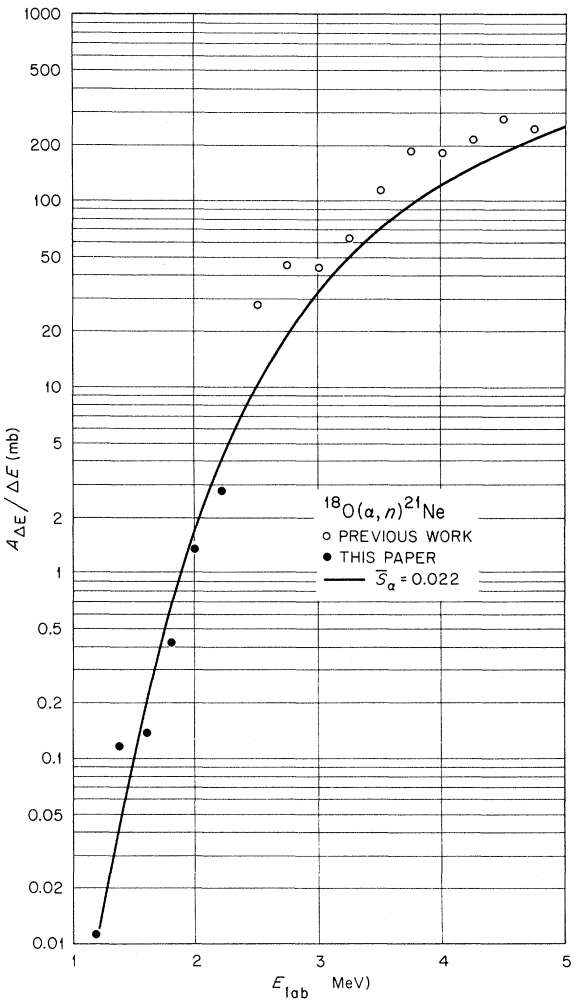

FIG. 11. Plot of $A_{\Delta E}/\Delta E$ as a function of incident α-particle energy for the reaction $^{18}O(\alpha,n)^{21}Ne$. $A_{\Delta E}$ is the area under the excitation curve in the energy region ΔE. The solid curve is calculated based on an α-particle strength function of $\bar{S}_\alpha = 0.022$. The open circles are from Ref. 8 and the closed circles are from the present work.

function, $\bar{S}_\alpha$, by

$$\frac{A_{\Delta E}}{\Delta E} = \frac{2\pi^2 \lambda^2}{2I+1} \sum (2J+1) \sum_{l=|J-I|}^{J+I} \frac{2kR}{A_l^2} \bar{S}_\alpha . \qquad (1)$$

Here $A_{\Delta E}/\Delta E$ is the unit area under the averaged yield curve and the other symbols have their usual meaning [the reaction radius was taken to be $1.4(A^{1/3}+1.59)$ fm]. Using Eq. (1), an $\bar{S}_\alpha$ was calculated for each energy increment, the average of these then is 0.029 ± 0.030 where the error is the variance for the different energy increments. The solid line of Fig. 8 is the calculation based on $\bar{S}_\alpha = 0.029$. As is seen, the fit to the data is not good, a result of the relative scarcity of available states in ^{17}O in the α-particle bombarding energy region around 4 MeV.

Davids[5] has made measurements of this reaction for bombarding α-particle energies of from 475 to 700 keV. When we use our value of $\bar{S}_\alpha$ and with the aid of Eq. (1) obtain extrapolated cross sections in this low-energy region we find that our values range from 5% higher at 700 keV to 33% higher at 475 keV. Such excellent agreement must be to some large extent fortuituous.

B. ^{17}O$(\alpha, n)^{20}$Ne

The points of Fig. 9 show the experimental data for the $^{17}(\alpha, n)^{20}$Ne reaction averaged over 400-keV energy intervals. As before, an $\bar{S}_\alpha = 0.030 \pm 0.023$ is obtained. The curve is from Eq. (1) using this value. The ^{17}O$(\alpha, n)^{20}$Ne cross section extrapolates to 10 nb at 750-keV bombarding energy and is falling at a rate of about a decade per 100 keV.

Very little high-resolution data are available in this region of excitation in ^{21}Ne. Unfortunately the 13-keV neutron total cross section data of Cohn and Fowler[22] overlap ours only at their highest level. Here their width, $\Gamma_{c.m.} \approx 9$ keV, and excitation energy, 8522 keV, are in excellent agreement with our values of 5 and 8524 keV, respectively.

In Fig. 10 we have used the data of Table II to plot the logarithm of the number of level spacings in $^{17}\text{O}+\alpha$ greater than some spacing D. If the distribution is random, such a plot gives a straight line, the negative reciprocal of whose slope should give the average level spacing and whose intercept should give the total number of levels. The result is that the intercept corresponds to 138 levels of which we experimentally observe 47 and that the slope corresponds to an average level spacing of 43 keV compared to our experimental value of 81 keV.

C. ^{18}O$(\alpha, n)^{21}$Ne

Figure 11 shows the data for the reaction ^{18}O$(\alpha, n)^{21}$Ne averaged over 400-keV intervals. The open points are from previous work at this laboratory[8] and the solid points are from the present experiment. A value of $S_\alpha = 0.022 \pm 0.010$ is obtained from the combined data. The ^{18}O$(\alpha, n)^{21}$Ne cross section extrapolates to a value of 140 nb at 900 keV (~50 keV above threshold) and at 1 MeV is 670 nb.

---

†Research sponsored by the U. S. Atomic Energy Commission under contract with Union Carbide Corporation and Monsanto Research Corporation.

[1]F. Ajzenberg-Selove, Nucl. Phys. A166, 1 (1971).
[2]J. L. Fowler, C. H. Johnson, and R. M. Feezel, to be published; C. H. Johnson, to be published.
[3]G. Chouraqui, Th. Muller, M. Port, and J. M. Thirion, J. Phys. (Paris) 31, 249 (1970).
[4]R. G. Couch and W. D. Arnette, to be published.
[5]C. N. Davids, Nucl. Phys. A110, 619 (1968).
[6]R. M. Williamson, T. Katman, and B. S. Burton, Phys. Rev. 117, 1325 (1964).
[7]M. K. Mehta, W. E. Hunt, H. S. Plendl, and R. H. Davis, Nucl. Phys. 48, 90 (1963).
[8]J. K. Bair and H. B. Willard, Phys. Rev. 128, 299 (1962).
[9]R. L. Macklin, Nucl. Instr. Methods 1, 335 (1957).
[10]J. L. Fowler and C. H. Johnson, Phys. Rev C 2, 124 (1970); and private communication.
[11]W. Whaling, in *Handbuch der Physik*, edited by S. Flügge (Springer-Verlag, Berlin, Germany, 1958), Vol. 34.
[12]R. B. J. Palmer, Proc. Phys. Soc. (London) 87, 681 (1966).
[13]D. I. Porat and K. Ramavataram, Proc. Roy. Soc. (London) 78, 1135 (1961).
[14]G. W. Kerr, J. M. Morris, and J. R. Risser, Nucl. Phys. A110, 637 (1968).
[15]K. K. Sekharan, A. S. Divatia, M. K. Mehta, S. S. Kerekatte, and K. B. Nambiar, Phys. Rev. 156, 1187 (1967).
[16]T. W. Bonner, A. A. Kraus, Jr., J. B. Marion, and J. P. Schiffer, Phys. Rev. 102, 1348 (1956).
[17]A. D. Robb, W. A. Schier, and E. Sheldon, Nucl. Phys. A147, 423 (1970).
[18]R. B. Walton, J. D. Clement, and F. Borelli, Phys. Rev. 107, 1065 (1957).
[18a]J. K. Bair, Nucl. Sci. Eng. (to be published).
[19]We would like to thank G. Alton of the Oak Ridge National Laboratory Isotopes Division for producing all of the "drive-in" targets used in this work.
[20]E. Selin, S. E. Arnell, and O. Almen, Nucl. Instr. Methods 56, 218 (1967).
[21]J. K. Bair, J. L. C. Ford, Jr., and C. M. Jones, Phys. Rev. 144, 799 (1966).
[22]H. O. Cohn and J. L. Fowler, Phys. Rev. 114, 194 (1959).